JOURNAL OF ENVIRONMENTAL SCIENCES 99 (2021) 260–266

Available online at www.sciencedirect.com

ScienceDirect

www.elsevier.com/locate/jes

JES JOURNAL OF ENVIRONMENTAL SCIENCES

www.jesc.ac.cn

Degradation of carbamazepine by MWCNTs-promoted generation of high-valent iron-oxo species in a mild system with O-bridged iron perfluorophthalocyanine dimers

*Zhiguo Zhao, Moyan Zhou, Nan Li, Yuyuan Yao, Wenxing Chen, Wangyang Lu**

National Engineering Lab for Textile Fiber Materials & Processing Technology (Zhejiang), Zhejiang Sci-Tech University, Hangzhou 310018, China

ARTICLE INFO

Article history:
Received 16 December 2019
Revised 1 July 2020
Accepted 3 July 2020
Available online 16 July 2020

Keywords:
$FePcF_{16}$-O-$FePcF_{16}$
Multi-walled carbon nanotubes
Synergistic catalytic
High-valent iron active species

ABSTRACT

Metal phthalocyanine has been extensively studied as a catalyst for degradation of carbamazepine (CBZ). However, metal phthalocyanine tends to undergo their own dimerization or polymerization, thereby reducing their activity points and affecting their catalytic properties. In this study, a catalytic system consisting of O-bridged iron perfluorophthalocyanine dimers ($FePcF_{16}$-O-$FePcF_{16}$), multi-walled carbon nanotubes (MWCNTs) and H_2O_2 was proposed. The results showed MWCNTs loaded with $FePcF_{16}$-O-$FePcF_{16}$ can achieve excellent degradation of CBZ with smaller dosages of $FePcF_{16}$-O-$FePcF_{16}$ and H_2O_2, and milder reaction temperatures. In addition, the results of experiments revealed the reaction mechanism of non-hydroxyl radicals. The highly oxidized high-valent iron-oxo (Fe(IV)=O) species was the main reactive species in the $FePcF_{16}$-O-$FePcF_{16}$/MWCNTs/H_2O_2 system. It is noteworthy that MWCNTs can improve the dispersion of $FePcF_{16}$-O-$FePcF_{16}$, contributing to the production of highly oxidized Fe(IV)=O. Then, the pathway of CBZ oxidative degradation was speculated, and the study results also provide new ideas for metal phthalocyanine-loaded carbon materials to degrade emerging pollutants.

Introduction

Pharmaceutical and personal care products (PPCPs) are widely used in daily life (Richardson et al., 2005), and have been detected as emerging organic pollutants in wastewater (Komesli et al., 2015). These contaminants are difficult to degrade when they have been present in the environment for a long time because of their strong polarity and biological activity (Yang et al., 2017; Gągol et al., 2018; Richardson and Ternes, 2014). In particular, carbamazepine (CBZ) is a typical PPCP and is one of the most frequently detected drug contaminants in the environment (Wang et al., 2017). Previous research has shown that CBZ is a common class of organic pollutants that is difficult to remove by conventional wastewater treatment (Clara et al., 2005). Therefore, CBZ is used as an artificial marker for studying environmental water pollution treatments (Wang et al., 2018; Li et al., 2019a; Keen et al., 2012).

Phthalocyanine, a biomimetic catalyst with strong catalytic properties, is a macrocyclic complex like porphyrin (Han et al., 2019; Li et al., 2019b; Zhao et al., 2018). It has received extensive attention in recent decades and is widely used in catalytic materials and other applications because of its low production cost and stable structure (Xu et al., 2016; Han et al., 2016). Recently, we reported the results of our study of the ox-

* Corresponding author.
E-mail: luwy@zstu.edu.cn (W. Lu).

https://doi.org/10.1016/j.jes.2020.07.004
1001-0742/

idative degradation of CBZ by an O-bridge iron perfluorophthalocyanine dimer ($FePcF_{16}$-O-$FePcF_{16}$) synthesized using the phthalonitrile method. In the $FePcF_{16}$-O-$FePcF_{16}$/H_2O_2 system, the catalyst exhibited excellent catalytic oxidation capacity in degradation experiments, with the reaction system achieving 100% degradation in 90 min. Afterwards, based on the results of a mechanism experiment, we speculated that the main active species in the reaction system is Fe(IV)=O. Lastly, the detected product was a small biodegradable molecule (Zhou et al., 2017). However, phthalocyanine compounds have strong associations with each other, and they tend to undergo their own dimerization or polymerization in the presence of a single catalyst, such that their solubility in organic solvents is extremely low (Sun et al., 2017a), thereby reducing their activity points and affecting their catalytic properties. Moreover, metal phthalocyanine is not conducive to recycling and may cause secondary pollution to the environment. To address the low catalytic activity and poor stability of phthalocyanine, attempts have been made to load phthalocyanine onto various materials to increase its solubility. In addition, the carrier can transport electrons during the catalytic reaction process (Gsanger et al., 2016; Huang et al., 2017a) and synergize with the phthalocyanine to improve its catalytic performance (Zhang et al., 2017).

Due to their unique tubular structures, carbon nanotubes have a high mechanical strength, large specific surface areas and excellent electrical conductivity (Yang et al., 2018). The high surface and surface-binding energies of carbon nanotubes means that they can adsorb and stuff particles, which means the active material can be better supported on the surface of the carbon nanotubes. As such, carbon nanotubes can be used as an excellent catalyst carrier (Luo et al., 2013; Ye et al., 2019). As carriers, carbon nanotubes can reduce the agglomeration of the catalyst powder, thereby increasing the activity and stability of the catalyst. Carbon nanotubes can also be used as an adsorbent to enrich a substrate (Xiong et al., 2018), and its good electrical properties can affect the catalytic reaction process and change the catalytic mechanism (Yao et al., 2016; Ma et al., 2015; Qin et al., 2018; Huang et al., 2017b). Some research results show that catalysts supported on carbon nanotubes exhibit excellent catalytic performances (Zhang et al., 2016, 2015; Osmieri et al., 2017). Therefore, we chose multi-walled carbon nanotubes (MWCNTs) as carriers to support O-bridge iron perfluorophthalocyanine dimers in the catalytic degradation of organic pollutants.

In this study, we synthesized an MWCNT loaded with $FePcF_{16}$-O-$FePcF_{16}$ ($FePcF_{16}$-O-$FePcF_{16}$/MWCNTs). The chemical structure of the catalyst and the amount of loaded $FePcF_{16}$-O-$FePcF_{16}$ were characterized and calculated by X-ray diffraction (XRD), Fourier transform infrared spectroscopy (FTIR), X-ray photoelectron spectroscopy (XPS), and inductively coupled plasma spectrometry (ICP). The performance of the $FePcF_{16}$-O-$FePcF_{16}$/MWCNTs catalytic system was determined based on the degradation of CBZ as the substrate, and the effects of different conditions on the degradation ability were investigated in the presence of H_2O_2. Compared with the $FePcF_{16}$-O-$FePcF_{16}$/H_2O_2 system, the influence of this carrier on the catalytic activity was explored and the optimal experimental conditions identified. Subsequently, based on a series of active-species detection experiments, we determined the main active species in the reaction system and inferred the possible catalytic reaction mechanism. Lastly, we examined the degradation products of CBZ by ultraperformance liquid chromatography (UPLC) and high-definition mass spectrometry (HDMS) and estimated the structural formula and possible degradation pathway of the product based on its molecular weight.

1. Materials and methods

1.1. Materials and reagents

Following the method reported in the literature (Zhou et al., 2017; Sun et al., 2017b; Gabrielov, 1994), we successfully prepared $FePcF_{16}$-O-$FePcF_{16}$. MWCNTs (95%), CBZ and isopropyl alcohol (IPA) were obtained from Aladdin Chemical Inc. (Shanghai, China). H_2O_2 was obtained from Sinopharm Chemical Reagent Co. (Shanghai, China), and 5,5-dimethyl-1-pyrroline-N-oxide (DMPO) was obtained from the J&K Chemical Co. All materials and reagents were of analytical grade and were used directly without secondary treatment.

1.2. Catalyst preparation

$FePcF_{16}$-O-$FePcF_{16}$/MWCNTs were prepared by placing 60 mg of $FePcF_{16}$-O-$FePcF_{16}$ and 600 mg of MWCNTs in a three-necked flask, pouring in 200 mL of absolute ethanol, and then condensing and refluxing this mixture at 80°C for 8 hr. The product was isolated by suction filtration and washed with absolute ethanol and ultrapure water until the filtrate was colorless. Finally, the obtained solid product was dried to obtain the $FePcF_{16}$-O-$FePcF_{16}$/MWCNT complex.

1.3. Characterization and analytical methods

The content of $FePcF_{16}$-O-$FePcF_{16}$ loaded onto the MWCNTs can be detected by inductive coupled plasma emission spectrometer (Varian 720-ES ICP-OES, Agilent, USA). To further determine the loading state of the $FePcF_{16}$-O-$FePcF_{16}$, Fourier transform infrared spectrometer (FTIR) (Thermo Nicolet 5700, Thermo, USA) spectrometer was used to collect the FTIR spectra of $FePcF_{16}$-O-$FePcF_{16}$, MWCNTs and $FePcF_{16}$-O-$FePcF_{16}$/MWCNTs. To characterize the structure of the catalyst, we used an XRD (D8 Discover, Bruker AXS, Germany) to irradiate the $FePcF_{16}$-O-$FePcF_{16}$, MWCNTs and $FePcF_{16}$-O-$FePcF_{16}$/MWCNTs from 5° to 70° under Cu-$K\alpha$ test conditions. To determine the loading state of phthalocyanine in more detail, the elemental composition of $FePcF_{16}$-O-$FePcF_{16}$/MWCNTs was identified by XPS ($K\alpha$, Thermo Fisher Scientific, USA).

1.4. Degradation experiment

We chose CBZ (2.5×10^{-5} mol/L) as the target substrate and H_2O_2 as the oxidant to study the catalytic activity of $FePcF_{16}$-O-$FePcF_{16}$/MWCNTs based on the CBZ degradation rate. In a general experiment, 20 mL of CBZ, 4 mg of $FePcF_{16}$-O-$FePcF_{16}$ and 5×10^{-3} mol/L of H_2O_2 were placed in a 40 mL sample bottle. The reaction was carried out at 30°C with high-speed stirring and the pH of the reaction solution was adjusted by adding H_2SO_4 or NaOH. At intervals, 1 mL of the test solution was taken from the reaction solution and filtered, and the concentration of CBZ was determined by ultraperformance liquid chromatography (UPLC) (HPLC, Waters, USA).

2. Results and discussion

2.1. Characterization the structure of $FePcF_{16}$-O-$FePcF_{16}$/MWCNTs

Based on the standard curve of Fe^{3+}, the load of the $FePcF_{16}$-O-$FePcF_{16}$ was 2.52×10^{-6} mol/g (Appendix A Fig. S1). It is worth

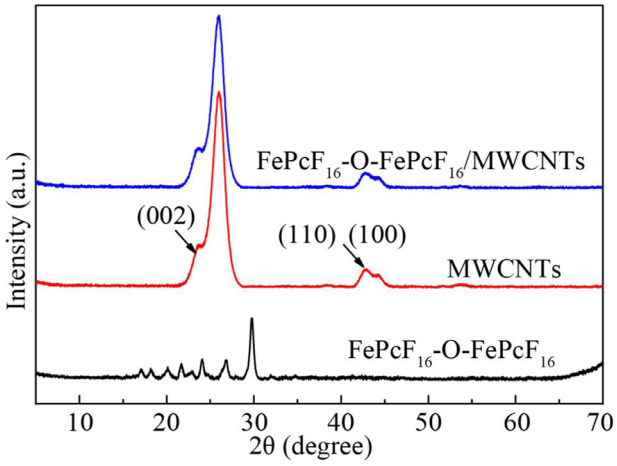

Fig. 1 – Powder X-ray diffraction diagrams of O-bridged iron perfluorophthalocyanine dimers ($FePcF_{16}$-O-$FePcF_{16}$), multi-walled carbon nanotubes (MWCNTs) and $FePcF_{16}$-O-$FePcF_{16}$/MWCNTs.

noting that the amount of catalyst used in the CBZ degradation experiment was 0.2 g/L, but the amount of $FePcF_{16}$-O-$FePcF_{16}$ calculated by ICP actually involved in the reaction was 8.7×10^{-4} g/L.

Fig. 1 shows the XRD patterns of $FePcF_{16}$-O-$FePcF_{16}$, MWCNTs and $FePcF_{16}$-O-$FePcF_{16}$/MWCNTs, respectively. Among them, the peak at $2\theta = 26°$ corresponds to the (002) lattice plane in the MWCNTs (Lin et al., 2010), and the peak around $2\theta = 43°$ corresponds to the graphite plane of (110) and (100). There were a series of diffraction peaks for the $FePcF_{16}$-O-$FePcF_{16}$. However, in the $FePcF_{16}$-O-$FePcF_{16}$/MWCNTs, these peaks disappeared, leaving only the corresponding MWCNT peaks. This indicates that the loading amount of $FePcF_{16}$-O-$FePcF_{16}$ was very low, and the characteristic diffraction peak of $FePcF_{16}$-O-$FePcF_{16}$ was difficult to detect with the instrument.

The infrared spectrum results are shown in Appendix A Fig. S2, in which the peak indicating the C-F stretching vibration at 2350 cm^{-1} is sufficient to confirm that $FePcF_{16}$-O-$FePcF_{16}$ was successfully loaded onto the MWCNTs.

The elemental composition was determined by XPS, which can further verify whether the catalyst has been successfully loaded (Cabana et al., 2015; He et al. 2018). The results show a peak that indicates the presence of fluorine in the $FePcF_{16}$-O-$FePcF_{16}$/MWCNTs (Appendix A Fig. S3). Based on the XPS broad–spectrum results, the narrow spectrum of each element is further examined.

Fig. 2b shows that the O 1s spectrum of the MWCNTs has one peak, which is presumed to be the C=O peak generated by surface oxidation, which is consistent with the C 1s spectrum of MWCNTs (Appendix A Fig. S4) (Luo et al., 2013). In Fig. 2c, there are peaks at 533.68 and 531.98 eV, which correspond to N-C=O and Fe-O bonds, respectively (Zhou et al., 2017; Yasuda et al., 2016). The absorption peak of $FePcF_{16}$-O-$FePcF_{16}$ at 530.68 eV is that of O in the oxygen bridge in dimerized perfluoroiron phthalocyanine. It can be seen in Fig. 2d that the type of O in $FePcF_{16}$-O-$FePcF_{16}$/MWCNTs is a combination of MWCNTs and $FePcF_{16}$-O-$FePcF_{16}$, which confirms that $FePcF_{16}$-O-$FePcF_{16}$ was successfully loaded onto the MWCNTs and that no new bond related to the O element was produced.

From the narrow spectrum of other elements, we obtained the same result (Appendix A Figs. S5, S6 and S7).

Based on the above analyses of various elements, we can conclude that $FePcF_{16}$-O-$FePcF_{16}$ was successfully loaded onto the MWCNTs.

2.2. *Oxidative degradation of CBZ*

To investigate CBZ degradation, a standard experiment explored the catalytic ability of the $FePcF_{16}$-O-$FePcF_{16}$/MWCNTs. CBZ was hardly degraded by H_2O_2 during 120 minutes of reaction time, and about 20% of the CBZ was adsorbed due to the adsorption capacity of MWCNTs when $FePcF_{16}$-O-$FePcF_{16}$/MWCNTs was present alone. However, all of the CBZ was degraded after 60 minutes when $FePcF_{16}$-O-$FePcF_{16}$/MWCNTs and H_2O_2 were both present (Fig. 3). Compared with pure $FePcF_{16}$-O-$FePcF_{16}$, the amount of $FePcF_{16}$-O-$FePcF_{16}$ in this experiment was greatly reduced and the reaction temperature was reduced to 303.15 K, which is sufficient to demonstrate that the introduction of MWCNTs greatly improved the oxidation performance of the catalyst.

2.2.1. *Influence of operational condition on treatment efficiency*

Different experimental conditions may affect the catalytic performance. Among them, temperature is an important parameter for both the reaction and adsorption processes.

As shown in Fig. 4, when no oxidant is present, the degradation rate of CBZ decreases with increases in temperature, which means that the higher the temperature, the higher is the desorption of the MWCNTs, and the less favorable the conditions for the adsorption of CBZ by the MWCNTs. In the presence of H_2O_2, the degradation rate of CBZ increases with temperature, and the CBZ is completely degraded by $FePcF_{16}$-O-$FePcF_{16}$ after a reaction time of 60 min at 60°C. However, compared to $FePcF_{16}$-O-$FePcF_{16}$, the supported catalyst can completely degrade CBZ over a wide temperature range within the same amount of time. Therefore, the introduction of MWCNTs not only greatly reduces the amount of catalyst, but also improves the catalytic ability, which means the reaction can completely degrade CBZ under mild conditions at a greatly reduced reaction temperature. The oxidative degradation rate of CBZ is already very high when the reaction temperature is 30°C, and subsequent increases in temperature yield no significant results, so 30°C was selected as the optimal temperature. Next, we calculated the value of the reaction rate constant k at different temperatures (Xun et al., 2015), and then determined the activation energy of the reaction is 40.16 kJ/mol (Appendix A Fig. S8).

Obviously, the degradation rate increased proportionally with increases in the H_2O_2 concentration in the $FePcF_{16}$-O-$FePcF_{16}$/H_2O_2 system (Fig. 5). However, to obtain the same degradation effect, the H_2O_2 concentration in the $FePcF_{16}$-O-$FePcF_{16}$/H_2O_2 system is 10 times that of the $FePcF_{16}$-O-$FePcF_{16}$/MWCNTs/H_2O_2 system. As the concentration of H_2O_2 increases, the catalyst does not activate all the H_2O_2 (Appendix A Fig. S9) (Monteagudo et al., 2015). The CBZ was completely degraded by H_2O_2 concentration of 5×10^{-3} mol/L. When the concentration of H_2O_2 was increased to 1×10^{-2} mol/L and then 2×10^{-2} mol/L, the CBZ was degraded in a shorter amount of time. Therefore, 5×10^{-3} mol/L was chosen as the optimal H_2O_2 concentration in subsequent experiments.

Next, the effect of solution pH (3, 5, 7, 9, and 11) on the degradation of CBZ by $FePcF_{16}$-O-$FePcF_{16}$/MWCNTs was investigated, and the results show that this system has a wide pH range, which differs from the optimum pH range (2–4) for the oxidation of organic compounds in a Fenton reaction (Appendix A Fig. S10) (Zhao et al., 2017).

2.2.2. *Oxidative activities of other organic pollutants*

To study the oxidizing ability of $FePcF_{16}$-O-$FePcF_{16}$/MWCNTs for other organic pollutant, we conducted experiments under the same experimental conditions and replaced the substrate CBZ with other common organic pollutants. As shown

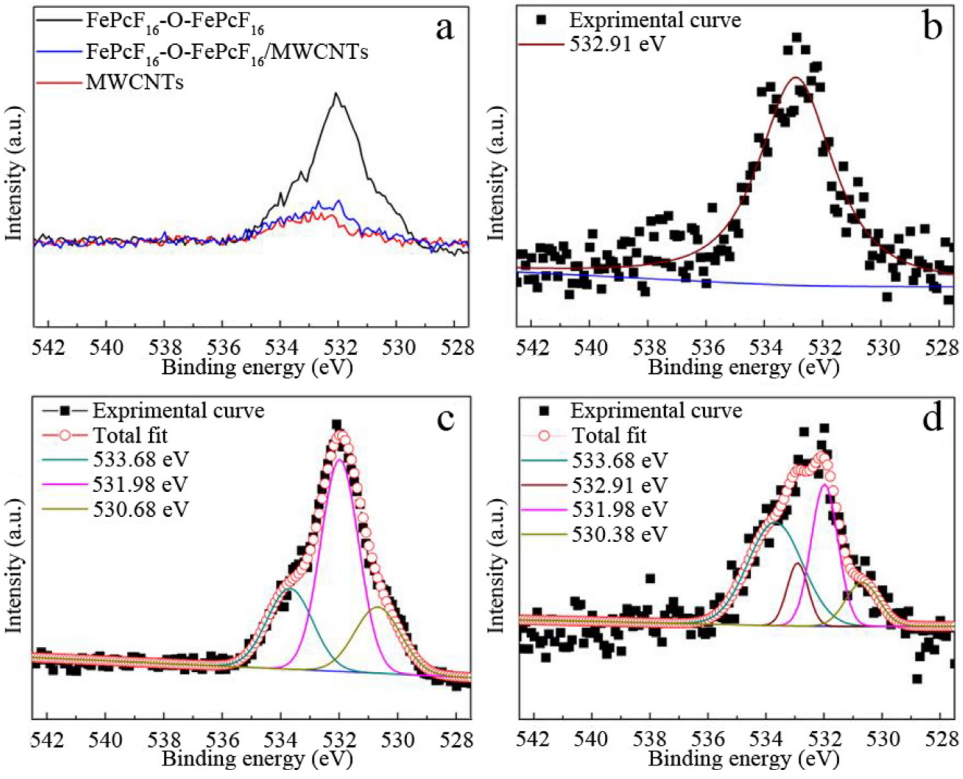

Fig. 2 – Curves of O1s peaks of (a) MWCNTs, $FePcF_{16}$-O-$FePcF_{16}$ and $FePcF_{16}$-O-$FePcF_{16}$/MWCNTs, (b) MWCNTs, (c) $FePcF_{16}$-O-$FePcF_{16}$ and (d) $FePcF_{16}$-O-$FePcF_{16}$/MWCNTs.

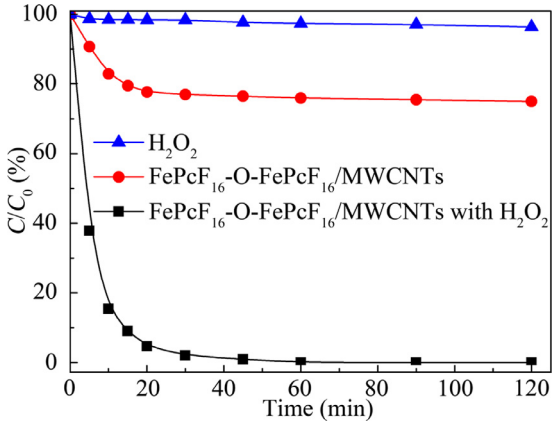

Fig. 3 – Degradation of carbamazepine (CBZ) under different conditions. Reaction conditions: $C_0 = 2.5 \times 10^{-5}$ mol/L, concentration of H_2O_2 ($[H_2O_2]$) = 5×10^{-3} mol/L, concentration of $FePcF_{16}$-O-$FePcF_{16}$/MWCNTs ([$FePcF_{16}$-O-$FePcF_{16}$/MWCNTs]) = 0.2 g/L, temperature (T) = 303.15 K and pH 7. C_0: initial concentration of CBZ; C: concentration of CBZ at time t.

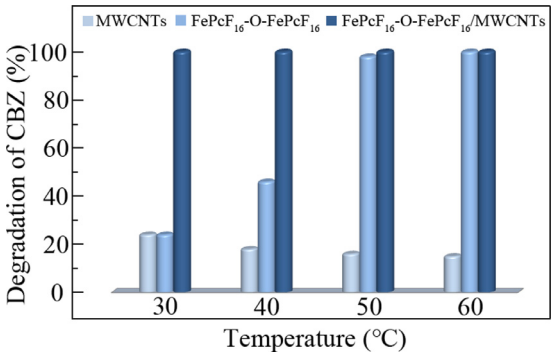

Fig. 4 – Degradation of CBZ under different conditions. Reaction conditions: $C_0 = 2.5 \times 10^{-5}$ mol/L, $[H_2O_2] = 2 \times 10^{-2}$ mol/L, pH 7, concentration of MWCNTs ([MWCNTs]) = 0.2 g/L or concentration of $FePcF_{16}$-O-$FePcF_{16}$ ([$FePcF_{16}$-O-$FePcF_{16}$]) = 0.1 g/L or [$FePcF_{16}$-O-$FePcF_{16}$/MWCNTs] = 0.2 g/L.

in Appendix A Table S1, the degradation rates of all the pollutants were greater than 90% in a short period of time, including dyes and drugs. These results show that $FePcF_{16}$-O-$FePcF_{16}$/MWCNTs also had a good oxidative degradation effect on other common organic pollutants. Therefore, we can conclude that this catalytic system has strong applicability in the degradation of organic pollutants.

2.2.3. *Reuse of catalyst*

Reuse performance and stability are two important factors for catalysts in practical applications. The degradation rate of CBZ can be greater than 90% after 10 cycles. Therefore, $FePcF_{16}$-O-$FePcF_{16}$/MWCNTs are reusable and maintain high catalytic activity (Appendix A Fig. S11).

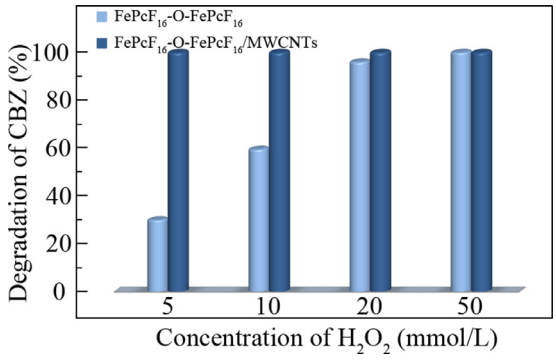

Fig. 5 – Effect of initial H_2O_2 concentration on catalytic degradation of CBZ different conditions. Reaction conditions: $C_0 = 2.5 \times 10^{-5}$ mol/L, T = 323.15 K, pH 7, [$FePcF_{16}$-O-$FePcF_{16}$] = 0.1 g/L or [$FePcF_{16}$-O-$FePcF_{16}$/MWCNTs] = 0.2 g/L.

2.3. *Mechanism analysis*

In the phthalocyanine/hydrogen peroxide system, the activation of hydrogen peroxide O-O bonds may follow one of two reaction pathways, and thereby generate either •OH or high-valent iron (IV) (Liu et al., 2017).

The electron paramagnetic resonance (EPR) spin-trapping technique, which can detect free radicals generated during CBZ degradation, was used to facilitate speculations about the experimental mechanism (Hu et al., 2016). As shown in Fig. 6a, unlike the set of quartets in standard Fenton reagents, the DMPO-•OH signal did not appear when $FePcF_{16}$-O-$FePcF_{16}$/MWCNTs was used as the catalyst. This indicates that the $FePcF_{16}$-O-$FePcF_{16}$/MWCNTs/H_2O_2 catalytic oxidation of the CBZ system produces very little •OH, which was hardly detectable by the instrument. Furthermore, •OH is not the main active center in the catalytic oxidation of the CBZ system by $FePcF_{16}$-O-$FePcF_{16}$/MWCNTs/H_2O_2. To investigate whether peroxygen free radicals may be produced in the oxidation system, Fig. 6b shows the results obtained under the same test conditions and with the water phase replaced by methanol. It is obvious that the DMPO-•OOH signal is also completely absent when $FePcF_{16}$-O-$FePcF_{16}$/MWCNTs is used as a catalyst. This result proves that •OOH is not the main active species in the $FePcF_{16}$-O-$FePcF_{16}$/MWCNTs/H_2O_2 system. In summary, the possibility that •OH and •OOH are the main active species is excluded, so Fe(IV)=O may be the main active species in this system. IPA inhibits oxidation reactions by its capture of •OH species, thereby changing the catalytic oxidation reaction of •OH as the active center, and affecting the oxidative degradation rate of CBZ. The experimental results show that •OH is not the main active center in the catalytic oxidation of the CBZ system of $FePcF_{16}$-O-$FePcF_{16}$/MWCNTs/H_2O_2 (Appendix A Fig. S12).

To determine the presence of high-valent iron, we conducted a dimethyl sulfoxide (DMSO) oxidation experiment, which is a method used to indirectly determine the presence of Fe(IV)=O. It can be seen from the following formula (2) that •OH cannot oxidize DMSO to dimethyl sulfone ($DMSO_2$), but DMSO can be oxidized to $DMSO_2$ by Fe(IV)=O (Chen et al., 2017; Pang et al., 2011). In the gas chromatograms in Fig. 7, we can see that the standard sample showed a unique peak indicating the presence of $DMSO_2$ at a retention time of 5.454 min. Similarly, the chromatogram of the oxidative degradation of the CBZ system by $FePcF_{16}$-O-$FePcF_{16}$/MWCNTs/H_2O_2 shows the only chromatographic peak indicating the presence

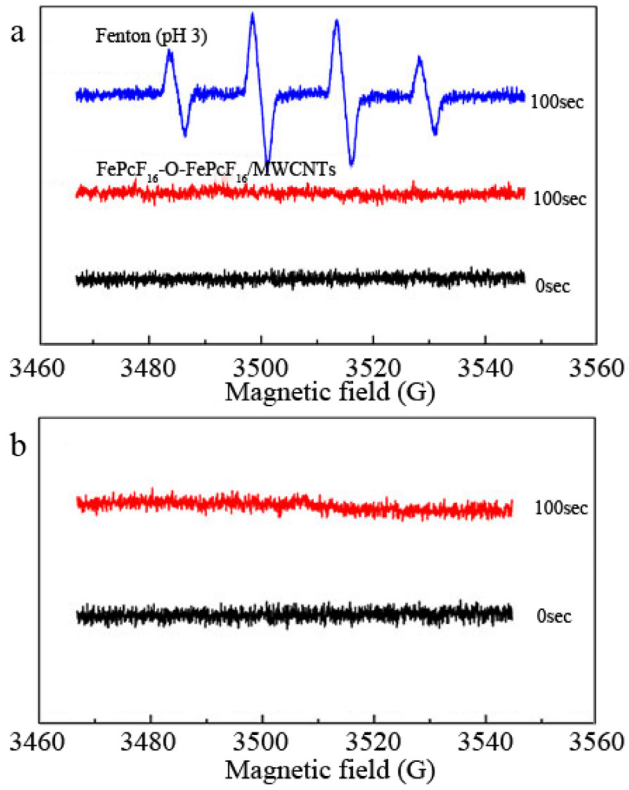

Fig. 6 – 5,5-Dimethyl-1-pyrroline N-oxide (DMPO) spin-trapping electron paramagnetic resonance (EPR) spectra in (a) pure aqueous solution or (b) methyl alcohol solutions with [H_2O_2] = 5×10^{-3} mol/L, concentration of DMPO ([DMPO]) = 5×10^{-3} mol/L, [$FePcF_{16}$-O-$FePcF_{16}$/MWCNTs] = 0.2 g/L.

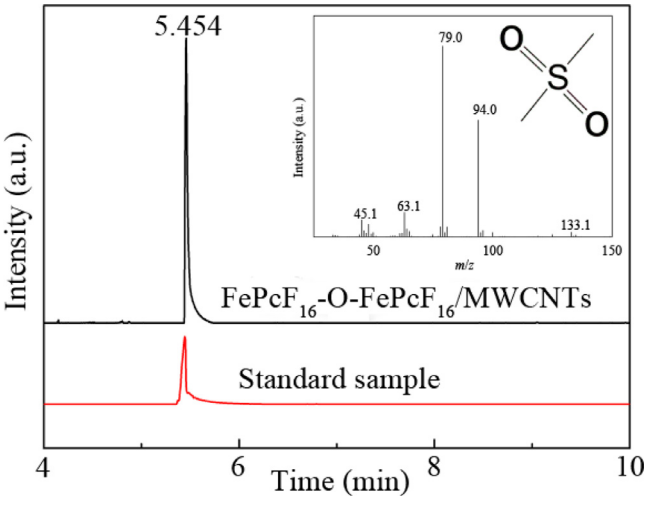

Fig. 7 – Gas chromatography mass spectrometry (GC-MS) chromatograms of dimethyl sulfone ($DMSO_2$) (1×10^{-3} mol/L), oxidation products of dimethyl sulfoxide (DMSO) catalyzed by $FePcF_{16}$-O-$FePcF_{16}$/MWCNTs. Inset shows the MS spectrum of $DMSO_2$. *m/z*: mass-to-charge ratio.

Table 1 – Oxidative degradation intermediates of CBZ examined by ultraperformance liquid chromatography-high-definition mass spectrometry (UPLC-HDMS).

Molecular formula	Retention time (min)	Theoretical mass (*m*/*z*)	Measured accurate (*m*/*z*)	Absolute error ($\times 10^{-3}$)
$C_{15}H_{12}N_2O$	4.81	237.1028	237.1032	0.4
$C_{15}H_{12}N_2O_2$	3.81	253.0977	253.0987	1.0
	4.05	253.0977	253.0979	0.2
	4.25	253.0977	253.0973	0.4
$C_{15}H_{10}N_2O_3$	2.80	267.0770	267.0765	0.5
	3.31	267.0770	267.0767	0.3
$C_{15}H_{12}N_2O_3$	3.02	269.0926	269.0919	0.5
$C_{14}H_9NO_2$	1.23	224.0712	224.0704	0.8
$C_{15}H_{10}N_2O_2$	4.17	251.0816	251.0811	0.5
$C_{13}H_9NO$	3.57	196.0762	196.0761	0.1

of $DMSO_2$ at the same retention time of 5.454 min. Therefore, we can speculate that the oxidative degradation of $FePcF_{16}$-O-$FePcF_{16}$/MWCNTs/H_2O_2 in the CBZ system is most likely due to the presence of Fe(IV)=O active species.

$$Fe(IV) = O + (CH_3)_2SO \rightarrow (CH_3)_2SO_2 \quad (1)$$

$$2 \bullet OH + 2(CH_3)_2SO + O_2 \rightarrow 2CH_3SO_2H + HCHO + CH_3OH \quad (2)$$

Peroxidase (POD) is an enzyme in which iron porphyrin is a prosthetic group and H_2O_2 is an electron acceptor. Colorless DPD can be oxidized to pink $DPD^{\bullet+}$ (Liu et al., 2014). Therefore, this reaction can be used to indirectly detect the presence of high-transition metals. The experimental results also proved that Fe(IV)=O is the main active substance (Appendix A Fig. S13).

Based on the experimental results, we speculate that the mechanism of the oxidative degradation of CBZ by the $FePcF_{16}$-O-$FePcF_{16}$/MWCNTs/H_2O_2 system, whereby MWCNTs act as electron transporters in the reaction system; thus, changing the electronic environment of $FePcF_{16}$-O-$FePcF_{16}$. For the catalytic mechanism process of $FePcF_{16}$-O-$FePcF_{16}$, the O-O bond of H_2O_2 has two fracture modes, i.e., homolysis or heterolysis, in different reaction conditions. In general, a heterolytically cleaved O-O bond causes the phthalocyanine to produce Fe(IV)=O active species, whereas when the O-O bond is cleaved homolytically, Fe(III)=O and •OH are produced in the reaction system. However, in the active species detection experiments, we could detect no generation of •OH. Therefore, we speculate that the Fe^{III}-O-Fe^{III}-OOH was cleaved heterolytically, which generates Fe^{IV}-O-Fe^{IV}=O at the same time as the loss of OH^- and degrades the CBZ into small molecules, which coincides with the experimental results. In summary, the $FePcF_{16}$-O-$FePcF_{16}$/MWCNTs/H_2O_2 system involves a non-radical reaction mechanism in the degradation of CBZ or organic pollutant systems, and Fe(IV)=O is the main active center.

2.4. *CBZ degradation products and pathways*

As shown in Table 1, we used UPLC-HDMS (Synapt G2-S HDMS, Waters, USA) in the positive ion detection mode to detect the intermediate product of CBZ in the degradation process, and identified all the intermediate products and their corresponding retention times, theoretical molecular masses and accurately measured masses. Based on the results, we speculate that the possible intermediate structure and degradation pathways are as shown in Fig. 8, whereby the double bond

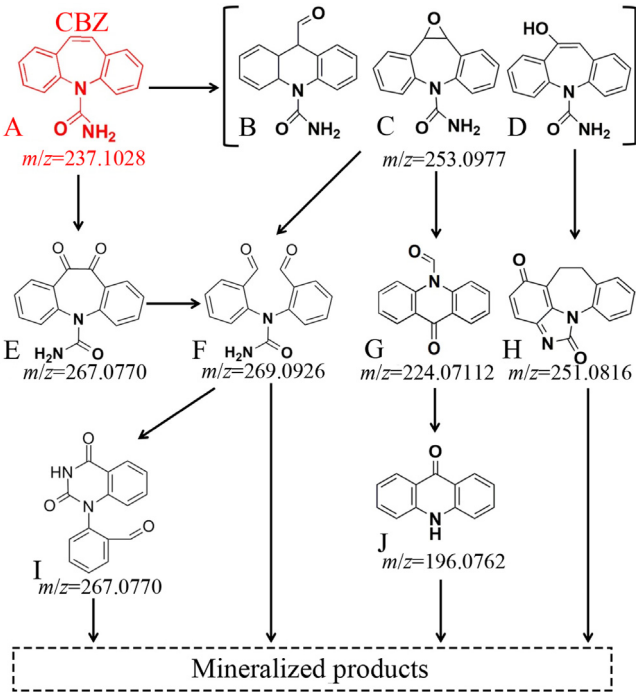

Fig. 8 – Proposed CBZ degradation pathway in the $FePcF_{16}$-O-$FePcF_{16}$/MWCNTs/H_2O_2 system.

on the central ring of CBZ is first attacked by Fe(IV)=O and converted into intermediate products (B, C, D) with mass to charge ratio (*m*/*z*) = 253.0977 and E (*m*/*z* = 267.0770) (Sun et al., 2013a). Then, a relatively gentle ring-shrinking reaction occurs in C, generating the intermediate product G (*m*/*z* = 224.0712), which is further oxidized to J (*m*/*z* = 196.0762). The intermediate product D undergoes intramolecular cyclization to H (*m*/*z* = 251.0816) (Sun et al., 2013b). The intermediate product F (*m*/*z* = 269.0926) is derived from the C10-C11 bond cleavage of E or further oxidation of C, and F continues to undergo an intramolecular reaction to convert to intermediate I (*m*/*z* = 267.0770) (Rao et al., 2013). Finally, the above intermediates and CBZ disappear, and no new product is formed, indicating that the $FePcF_{16}$-O-$FePcF_{16}$/MWCNTs/H_2O_2 system can effectively transform and degrade CBZ and its intermediates, mineralizing them into small molecules.

3. Conclusions

In conclusion, $FePcF_{16}$-O-$FePcF_{16}$ was successfully loaded onto MWCNTs. Experimental results showed that loading $FePcF_{16}$-O-$FePcF_{16}$ on MWCNTs reduced the amount of $FePcF_{16}$-O-$FePcF_{16}$ and H_2O_2, and reduced the activation energy of the reaction. Sufficient evidence shows that MWCNTs can improve the dispersion of $FePcF_{16}$-O-$FePcF_{16}$, contributing to produce Fe(IV)=O reactive site. Furthermore, the degradation pathway of CBZ was analyzed by UPLC-HDMS. In summary, this work provides new insights regarding the loading of catalysts and the degradation of organic pollutants.

Declaration of competing interest

The authors declare that they have no known competing financial interests or personal relationships that could have appeared to influence the work reported in this paper.

Acknowledgments

This work was supported by the National Natural Science Foundation of China (No. 51703201) and Zhejiang Provincial Natural Science Foundation of China (No. LQ17E030003).

Appendix A. Supplementary data

Supplementary material associated with this article can be found in the online version at doi:10.1016/j.jes.2020.07.004.

REFERENCES

Cabana, L., Ke, X., Kepić, D., Oro-Solé, J., Tobías-Rossell, E., Van Tendeloo, G., et al., 2015. The role of steam treatment on the structure, purity and length distribution of multi-walled carbon nanotubes. Carbon 93, 1059–1067.

Chen, X., Lu, W., Xu, T., Li, N., Zhu, Z., Wang, G., et al., 2017. Visible-light-assisted generation of high-valent iron-oxo species anchored axially on g-C_3N_4 for efficient degradation of organic pollutants. Chem. Eng. J. 328, 853–861.

Clara, M., Strenn, B., Gans, O., Martinez, E., Kreuzinger, N., Kroiss, H., 2005. Removal of selected pharmaceuticals, fragrances and endocrine disrupting compounds in a membrane bioreactor and conventional wastewater treatment plants. Water Res. 39 (19), 4797–4807.

Gabrielov, A.G., Bell, S.L., Bediouib, F., Devynckb, J., 1994. Faujasite-type zeolites modified with iron perfluorophthalocyanines: synthesis and characterization. Micropor. Mater. 2 (1994), 119–126.

Gągol, M., Przyjazny, A., Boczkaj, G., 2018. Wastewater treatment by means of advanced oxidation processes based on cavitation – a review. Chem. Eng. J. 338, 599–627.

Gsanger, M., Bialas, D., Huang, L., Stolte, M., Wurthner, F., 2016. Organic semiconductors based on dyes and color pigments. Adv. Mater. 28 (19), 3615–3645.

Han, Z., Han, X., Zhao, X., Yu, J., Xu, H., 2016. Iron phthalocyanine supported on amidoximated PAN fiber as effective catalyst for controllable hydrogen peroxide activation in oxidizing organic dyes. J. Hazard. Mater. 320, 27–35.

Han, Z., Li, J., Han, X., Ji, X., Zhao, X., 2019. A comparative study of iron-based PAN fibrous catalysts for peroxymonosulfate activation in decomposing organic contaminants. Chem. Eng. J. 358, 176–187.

He, Y., Yang, S., Liu, H., Shao, Q., Chen, Q., Lu, C., et al., 2018. Reinforced carbon fiber laminates with oriented carbon nanotube epoxy nanocomposites: magnetic field assisted alignment and cryogenic temperature mechanical properties. J. Colloid. Interf. Sci. 517, 40–51.

Hu, J., Liu, H., Wang, L., Li, N., Xu, T., Lu, W., et al., 2016. Electronic properties of carbon nanotubes linked covalently with iron phthalocyanine to determine the formation of high-valent iron intermediates or hydroxyl radicals. Carbon 100, 408–416.

Huang, W., Ahlfield, J.M., Kohl, P.A., Zhang, X., 2017a. Heat treated tethered iron phthalocyanine carbon nanotube-based catalysts for oxygen reduction reaction in hybrid fuel cells. Electrochim. Acta 257, 224–232.

Huang, J., Yuan, Y., Shao, Y., Yan, Y., 2017b. Understanding the physical properties of hybrid perovskites for photovoltaic applications. Nat. Rev. Mater. 2, 17042.

Keen, O.S., Baik, S., Linden, K.G., Aga, D.S., Love, N.G., 2012. Enhanced biodegradation of carbamazepine after UV/H_2O_2 advanced oxidation. Environ. Sci. Technol. 46 (11), 6222–6227.

Komesli, O.T., Muz, M., Ak, M.S., Bakırdere, S., Gokcay, C.F., 2015. Occurrence, fate and removal of endocrine disrupting compounds (EDCs) in Turkish wastewater treatment plants. Chem. Eng. J. 277, 202–208.

Li, S., Wang, Z., Zhao, X., Yang, X., Liang, G., Xie, X., 2019a. Insight into enhanced carbamazepine photodegradation over biochar-based magnetic photocatalyst Fe_3O_4/BiOBr/BC under visible LED light irradiation. Chem. Eng. J. 360, 600–611.

Li, X., Zheng, B.D., Peng, X.H., Li, S.Z., Ying, J.W., Zhao, Y., et al., 2019b. . Phthalocyanines as medicinal photosensitizers: developments in the last five years. Coordin. Chem. Rev. 379, 147–160.

Lin, C.K., Wu, C.H., Tsai, C.Y., Chen, C.Y., Wang, S.C., 2010. Pseudocapacitive performance of hybrid manganese oxide films with multiwalled-CNT additions. Surf. Coat. Tech. 205 (5), 1595–1598.

Liu, H., Bao, S., Cai, Z., Xu, T., Li, N., Wang, L., et al., 2017. A novel method for ultra-deep desulfurization of liquid fuels at room temperature. Chem. Eng. J. 317, 1092–1098.

Liu, X., Fan, J.H., Hao, Y., Ma, L.M., 2014. The degradation of EDTA by the bimetallic Fe–Cu/O_2 system. Chem. Eng. J. 250, 354–365.

Luo, C., Tian, Z., Yang, B., Zhang, L., Yan, S., 2013. Manganese dioxide/iron oxide/acid oxidized multi-walled carbon nanotube magnetic nanocomposite for enhanced hexavalent chromium removal. Chem. Eng. J. 234, 256–265.

Ma, J., Yang, M., Yu, F., Chen, J., 2015. Easy solid-phase synthesis of pH-insensitive heterogeneous CNTs/FeS Fenton-like catalyst for the removal of antibiotics from aqueous solution. J. Colloid. Interf. Sci. 444, 24–32.

Monteagudo, J.M., Durán, A., González, R., Expósito, A.J., 2015. In situ chemical oxidation of carbamazepine solutions using persulfate simultaneously activated by heat energy, UV light, Fe^{2+} ions, and H_2O_2. Appl. Catal. B-Environ. 176-177, 120–129.

Osmieri, L., Escudero-Cid, R., Armandi, M., Videla, M., García, A.H.A., Fierro, J.L., Ocón, P., et al., 2017. Fe-N/C catalysts for oxygen reduction reaction supported on different carbonaceous materials. Performance in acidic and alkaline direct alcohol fuel cells.. Appl. Catal. B-Environ. 205, 637–653.

Pang, S.Y., Jiang, J., Ma, J., 2011. Oxidation of sulfoxides and arsenic(III) in corrosion of nanoscale zero valent iron by oxygen: evidence against ferryl ions(Fe(IV)) as active intermediates in Fenton reaction. Environ. Sci. Technol. 45, 307–312.

Qin, Y., Li, G., Gao, Y., Zhang, L., Ok, Y.S., An, T., 2018. Persistent free radicals in carbon-based materials on transformation of refractory organic contaminants (ROCs) in water: a critical review. Water Res. 137, 130–143.

Rao, Y.F., Chu, W., Wang, Y.R., 2013. Photocatalytic oxidation of carbamazepine in triclinic-WO_3 suspension: tole of alcohol and sulfate radicals in the degradation pathway. Appl. Catal. A-Gen. 468, 240–249.

Richardson, B.J., Lam, P.K., Martin, M., 2005. Emerging chemicals of concern: pharmaceuticals and personal care products (PPCPs) in Asia, with particular reference to Southern China. Mar. Pollut. Bull. 50 (9), 913–920.

Richardson, S.D., Ternes, T.A., 2014. Water analysis: emerging contaminants and current issues. Anal. Chem. 86 (6), 2813–2848.

Sun, S.P., Zeng, X., Lemley, A.T., 2013a. Kinetics and mechanism of carbamazepine degradation by a modified Fenton-like reaction with ferric-nitrilotriacetate complexes. J. Hazard. Mater. 252-253, 155–165.

Sun, S.P., Zeng, X., Lemley, A.T., 2013b. Nano-magnetite catalyzed heterogeneous Fenton-like degradation of emerging contaminants carbamazepine and ibuprofen in aqueous suspensions and montmorillonite clay slurries at neutral pH. J. Mol. Catal -Chem. 371, 94–103.

Sun, Y., Hu, H., Zhao, N., Xia, T., Yu, B., Shen, C., et al., 2017a. Multifunctional polycationic photosensitizer conjugates with rich hydroxyl groups for versatile water-soluble photodynamic therapy nanoplatforms. Biomaterials 117, 77–91.

Sun, Y.L., Li, X.G., Wang, S.R., Zhang, L.J., Ma, F., 2017b. Synthesis, spectral properties of zinc hexadecafluorophthalocyanine ($ZnPcF_{16}$) and its application in organic thin film transistors. Mater. Trans. 58 (1), 103–106.

Wang, W.L., Wu, Q.Y., Li, Z.M., Lu, Y., Du, Y., Wang, T., et al., 2017. Light-emitting diodes as an emerging UV source for UV/chlorine oxidation: carbamazepine degradation and toxicity changes. Chem. Eng. J. 310, 148–156.

Wang, W.L., Wu, Q.Y., Du, Y., Huang, N., Hu, H.Y., 2018. Elimination of chlorine-refractory carbamazepine by breakpoint chlorination: reactive species and oxidation byproducts. Water Res. 129, 115–122.

Xiong, W., Zeng, Z., Li, X., Zeng, G., Xiao, R., Yang, Z., et al., 2018. Multi-walled carbon nanotube/amino-functionalized MIL-53(Fe) composites: remarkable adsorptive removal of antibiotics from aqueous solutions. Chemosphere 210, 1061–1069.

Xu, T., Ni, D., Chen, X., Wu, F., Ge, P., Lu, W., et al., 2016. Self-floating graphitic carbon nitride/zinc phthalocyanine nanofibers for photocatalytic degradation of contaminants. J. Hazard. Mater. 317, 17–26.

Xun, S., Zhu, W., Zhu, F., Chang, Y., Zheng, D., Qin, Y., et al., 2015. Design and synthesis of W-containing mesoporous material with excellent catalytic activity for the oxidation of 4,6-DMDBT in fuels. Chem. Eng. J. 280, 256–264.

Yang, Y., Ok, Y.S., Kim, K.H., Kwon, E.E., Tsang, Y.F., 2017. Occurrences and removal of pharmaceuticals and personal care products (PPCPs) in drinking water and water/sewage treatment plants: a review. Sci. Total. Environ. 596-597, 303–320.

Yang, Z., Yu, A., Shan, C., Gao, G., Pan, B., 2018. Enhanced Fe(III)-mediated Fenton oxidation of atrazine in the presence of functionalized multi-walled carbon nanotubes. Water Res. 137, 37–46.

Yao, Y., Chen, H., Qin, J., Wu, G., Lian, C., Zhang, J., et al., 2016. Iron encapsulated in boron and nitrogen codoped carbon nanotubes as synergistic catalysts for Fenton-like reaction. Water Res. 101, 281–291.

Yasuda, S., Furuya, A., Uchibori, Y., Kim, J., Murakoshi, K., 2016. Iron-nitrogen-doped vertically aligned carbon nanotube electrocatalyst for the oxygen reduction reaction. Adv. Funct. Mater. 26 (5), 738–744.

Ye, S., Zhou, X., Xu, Y., Lai, W., Yan, K., Huang, L., et al., 2019. Photocatalytic performance of multi-walled carbon nanotube/$BiVO_4$ synthesized by electro-spinning process and its degradation mechanisms on oxytetracycline. Chem. Eng. J. 373, 880–890.

Zhang, G., Li, Z., Zheng, H., Fu, T., Ju, Y., Wang, Y., 2015. Influence of the surface oxygenated groups of activated carbon on preparation of a nano Cu/AC catalyst and heterogeneous catalysis in the oxidative carbonylation of methanol. Appl. Catal. B-Environ. 179, 95–105.

Zhang, X., Wu, Z., Zhang, X., Li, L., Li, Y., Xu, H., et al., 2017. Highly selective and active CO_2 reduction electrocatalysts based on cobalt phthalocyanine/carbon nanotube hybrid structures. Nat. Commun. 8, 14675.

Zhang, X., Feng, M., Qu, R., Liu, H., Wang, L., Wang, Z., 2016. Catalytic degradation of diethyl phthalate in aqueous solution by persulfate activated with nano-scaled magnetic $CuFe_2O_4$/MWCNTs. Chem. Eng. J. 301, 1–11.

Zhao, H., Chen, Y., Peng, Q., Wang, Q., Zhao, G., 2017. Catalytic activity of MOF(2Fe/Co)/carbon aerogel for improving H_2O_2 and •OH generation in solar photo–electro–Fenton process. Appl. Catal. B-Environ. 203, 127–137.

Zhao, Y.M., Yu, G.Q., Wang, F.F., Wei, P.J., Liu, J.G., 2018. Bioinspired transition-metal complexes as electrocatalysts for the oxygen reduction reaction. Chem. Eur. J. 25 (15), 3726–3739.

Zhou, J., Wu, F., Zhu, Z., Xu, T., Lu, W., 2017. Identification of O-bridge iron perfluorophthalocyanine dimer and generation of high-valent diiron-oxo species for the oxidation of organic pollutants. Chem. Eng. J. 328, 915–926.